JACS
JOURNAL OF THE AMERICAN CHEMICAL SOCIETY

Communication

pubs.acs.org/JACS

Molecular Optimization Enables over 13% Efficiency in Organic Solar Cells

Wenchao Zhao,[†,‡] Sunsun Li,[†,‡] Huifeng Yao,[*,†,‡] Shaoqing Zhang,[†,‡] Yun Zhang,[†,‡] Bei Yang,[†,‡] and Jianhui Hou[*,†,‡]

[†]Beijing National Laboratory for Molecular Sciences, State Key Laboratory of Polymer Physics and Chemistry, CAS Research/Education Center for Excellence in Molecular Sciences, Institute of Chemistry, Chinese Academy of Sciences, Beijing 100190, China

[‡]University of Chinese Academy of Sciences, Beijing 100049, China

Supporting Information

ABSTRACT: A new polymer donor (PBDB-T-SF) and a new small molecule acceptor (IT-4F) for fullerene-free organic solar cells (OSCs) were designed and synthesized. The influences of fluorination on the absorption spectra, molecular energy levels, and charge mobilities of the donor and acceptor were systematically studied. The PBDB-T-SF:IT-4F-based OSC device showed a record high efficiency of 13.1%, and an efficiency of over 12% can be obtained with a thickness of 100−200 nm, suggesting the promise of fullerene-free OSCs in practical applications.

Organic solar cells (OSCs) have attracted considerable attention as a clean-energy harvesting technology for their ability to form flexible, large-area photovoltaic panels by low-cost solution processing methods.[1−4] The highly tunable optoelectronic properties of organic photovoltaic materials have enabled the precise optimization of absorption spectra, molecular energy levels, and charge mobilities of the resulting electron donor and acceptor materials, and thus an improved open-circuit voltage (V_{OC}), short circuit current density (J_{SC}), and fill factor (FF) can be achieved in the corresponding OSC devices.[5] Fullerene derivatives, such as PC71BM ([6,6]-phenylC71butyric acid methyl ester) and ICBA (indene-C_{60} bisadduct), are the most widely used acceptor materials in OSCs,[6,7] and numerous works have focused on the design of highly efficient donors, leading to devices with power conversion efficiencies (PCEs) of over 11%.[8−11] However, further improvements in efficiency face great challenges, as fullerene-based OSCs suffer from large energy losses.[12] Recently, nonfullerene small molecules have emerged as very promising electron acceptors in OSCs, and PCEs of over 12% have been recorded.[13] It is of great importance to improve further the efficiency of nonfullerene OSCs via fine molecular design strategies.[14−24]

Over the past decades, many efficient molecular design strategies have been developed to tune the optoelectronic properties of photovoltaic materials, such as donor−acceptor structure modifications, side chain engineering and functional group modulations.[25−27] Molecular frontier orbits, including the density distribution of π-electrons and their energy levels, and intermolecular interactions can be tuned efficiently via these practical chemical modulations. Among which, the introduction of fluorine, which is the most electronegative atom with the smallest size in the periodic table, is very useful for the molecular design of photovoltaic molecules.[28−33] Fluorinated organic semiconductor molecules have several advantages. First, fluorination simultaneously down-shifts the highest occupied molecular orbital (HOMO) and the lowest unoccupied molecular orbital (LUMO) levels without causing strong steric hindrance of the resulting molecules.[29,30] Second, enhanced inter/intramolecular interactions are often observed in fluorinated molecules due to the noncovalent interactions of F···H, S···F, and so on, which improve their crystallinity and hence facilitate charge transport.[31] Third, fluorinated molecules show higher polarization and a reduced Coulombic potential between holes and electrons.[32] In addition, fluorinated semiconductors sometimes have higher absorption coefficients than their nonfluorinated counterparts.[33] At present, state-of-the-art fullerene-based OSCs are fabricated from fluorinated polymer or small molecule donors, and PCEs over 11% have been obtained.[10,11] Our recent works have demonstrated that nonfullerene OSCs fabricated by the polymer donor PBDB-T and the small molecular acceptor ITIC could yield PCEs 0f over 11%.[34,35] To improve further the efficiencies of the OSCs, we optimized PBDB-T and ITIC separately by introducing alkylthio and methyl groups, respectively, and the PCEs of the resulting OSCs were increased to over 12%.[13] For nonfullerene OSCs, fluorination is a very promising molecular design strategy to improve further the photovoltaic performance.[19,36] Importantly, since the fluorination of acceptors results in down-shifted LUMO energy levels, synergistic molecular modification of the donors must be considered to avoid decreases in the V_{OC} of the OSCs.

Here, we perform the rational molecular optimization of PBDB-T and ITIC via fluorination to enhance the photovoltaic performance of the resulting OSCs. Both the newly prepared polymer donor PBDB-T-SF and small molecular acceptor IT-4F (Figure 1) show down-shifted molecular energy levels compared with their nonfluorinated counterparts. Both the optimized donor and acceptor display higher absorption coefficients relative to their previously reported counterparts. Moreover, IT-4F shows a more red-shifted absorption

Received: March 21, 2017
Published: May 17, 2017

DOI: 10.1021/jacs.7b02677
J. Am. Chem. Soc. 2017, 139, 7148−7151

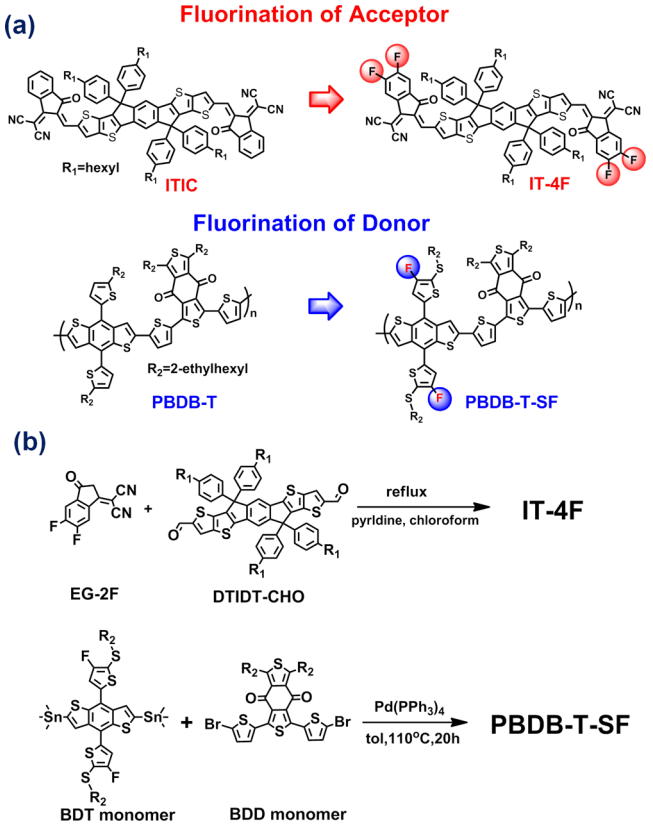

Figure 1. (a) Molecular structure of the fluorinated donor and acceptor. (b) Synthetic procedure of the fluorinated donor and acceptor.

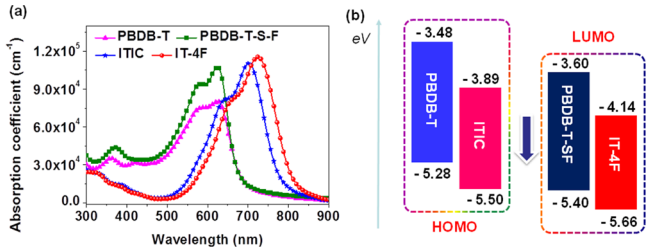

Figure 2. (a) Absorption spectra and (b) molecular energy levels of the donors and acceptors.

spectrum than ITIC, whereas the donors possess almost the same absorption bandgaps. Impressively, a certified PCE of 13% was obtained with the PBDB-T-SF:IT-4F-based OSC device, which to the best of our knowledge, is the highest value reported in the literature to date for OSCs.

As shown in Figure 1, the target products PBDB-T-SF and IT-4F were prepared by Stille coupling and Knoevenagel condensation reactions, respectively. The detailed synthetic procedures are provided in the Experimental Section of the Supporting Information. Both the donor and acceptor can be dissolved in common solvents, such as chloroform, chlorobenzene, and *o*-dichlorobenzene. For the new polymer, gel permeation chromatography (GPC) gives a number-average molecular weight (M_n) of 20.9 kDa with a polydispersity index (PDI) of 3.51. Theoretical calculations using density functional theory (Figure S1) suggest that the newly designed donor and acceptor have molecular configurations and wave function distributions of their frontier orbitals that are similar to those of their counterparts. Both the HOMO and LUMO energy levels were down-shifted.

The absorption spectra of solid thin films of the polymer donors and nonfullerene acceptors are shown in Figure 2a. The polymer donors show almost the same absorption onsets at approximately 688 nm, corresponding to an optical band gap of 1.80 eV. Notably, the main peak of the PBDB-T-SF film at 626 nm is clearly enhanced compared to that of the PBDB-T film, which suggests strong $\pi-\pi$ intermolecular interactions occur after molecular modification. The maximum absorption coefficient (1.08×10^5 cm^{-1}) of the PBDB-T-SF film is enhanced by ca. 34% compared with that of the PBDB-T film.

For the small molecular acceptors, in comparison with ITIC, not only is the absorption coefficient improved for IT-4F (1.16×10^5 cm^{-1} for IT-4F and 1.10×10^5 cm^{-1} for ITIC; in chloroform solutions, the absorption coefficient of ITIC and IT-4F are 1.90×10^5 and 2.10×10^5 M^{-1} cm^{-1}, respectively, Figure S2) but also the absorption main peak is red-shifted by 17 nm, which can be ascribed to enhanced intramolecular charge transfer (Table 1). When PBDB-T-SF and IT-4F are

Table 1. Physical, Electronic, and Optical Properties of the Donors and Acceptors

Materials	λ_{max}[a] (nm)	ε_{max}[a] (10^5 cm^{-1})	HOMO[b] (eV)	LUMO[b] (eV)
PBDB-T	626	0.80	−5.28	−3.48
PBDB-T-SF	626	1.08	−5.40	−3.60
ITIC	700	1.10	−5.50	−3.89
IT-4F	717	1.16	−5.66	−4.14

[a]Thin film spin-coated from chloroform solution. [b]Obtained from the ultraviolet photoelectron spectroscopy (UPS) results.

blended as the active layer for OSCs, the broader optical absorption band and higher absorption coefficient are helpful for harvesting more solar photons, and thus an increased J_{SC} can be expected. X-ray diffraction (XRD) (Figure S3) was used to investigate the influence of fluorination on the crystalline properties of the donors and acceptors. In comparison with PBDB-T and ITIC, the PBDB-T-SF and IT-4F films show more ordered intermolecular arrangements. In addition, the hole mobilities of PBDB-T and PBDB-T-SF and the electron mobilities of ITIC and IT-4F were investigated using the space-charge-limited current (SCLC) method. The results (Table S1) indicate that the hole mobility (μ_h) of PBDB-T-SF and the electron mobility (μ_e) of IT-4F were slightly improved.

The molecular energy levels of the donors and acceptors were measured in parallel via ultraviolet photoelectron spectroscopy (UPS) (Figure S4). As shown in Figure 2b and Table 1, the HOMO/LUMO levels of PBDB-T, ITIC, PBDB-T-SF and IT-4F are −5.28/−3.48 eV, − 5.50/−3.89 eV, −5.40/−3.60 eV, and −5.66/−4.14 eV, respectively. The overall down-shift of the molecular energy levels of the donors and acceptors will not lead to considerable differences in the V_{OC} of the OSCs, and sufficient driving forces for efficient exciton separation are retained. Moreover, the low-lying HOMO and LUMO levels of PBDB-T-SF and IT-4F may have certain advantages, such as good chemical stability and large polarization, which is beneficial for improving their photovoltaic performance.

We then fabricated OSC devices with an inverted structure of indium tin oxide (ITO)/ZnO/active layer/MoO_3/Al to investigate the photovoltaic performance of the PBDB-T-

DOI: 10.1021/jacs.7b02677
J. Am. Chem. Soc. 2017, 139, 7148−7151

SF:IT-4F blend, and the device processing conditions were similar to those of PBDB-T:ITIC reported in our previous work.[34] The current density−voltage (J−V) curves are displayed in Figure 3a. In comparison with the control device

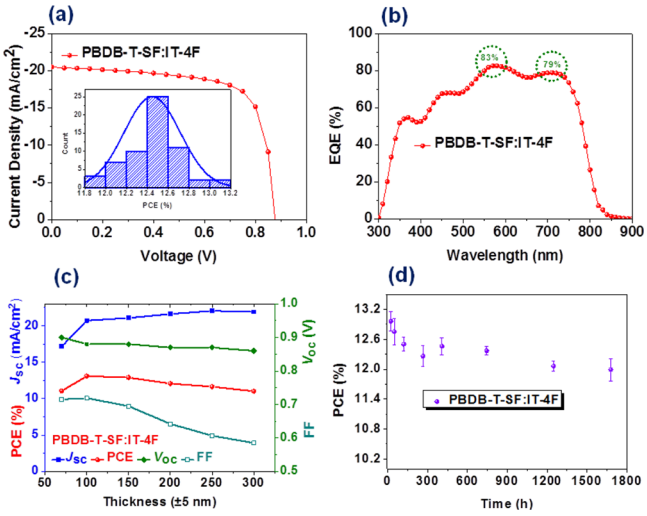

Figure 3. (a) J−V curve and histogram (inset) of the PCE measurements for 60 PBDB-T-SF:IT-4F-based cells; (b) EQE curve and (c) device performance parameters (PCE, J_{SC}, V_{OC}, and FF) versus the active layer thickness. (d) Storage stability of the PBDB-T-SF:IT-4F-based OSCs.

fabricated from PBDB-T:ITIC (Figure S5a), the PBDB-T-SF:IT-4F-based OSC showed a significant improvement in the J_{SC} from 17.03 to 20.50 mA/cm^2 due to the broad absorption range and enhanced absorption coefficient of the active layer, whereas the V_{OC} (0.88 V) and FF (0.719) did not change much (Table S2). The energy losses ($E_g^{opt} - eV_{OC}$) of the PBDB-T-SF:IT-4F-based device (0.66 eV) has some decrease when compared with than of PBDB-T:ITIC-based device (0.69 eV). Consequently, an impressive PCE of 13.0% was recorded for the PBDB-T-SF:IT-4F-based device, which was certified as 13.1% by the National Institute of Metrology, China (NIM), suggesting that the results obtained in our lab are reliable (Figure S6 and Figure S7a). What's more, 1.00 cm^2 cell was fabricated and showed a PCE of 11.1%, which also has been certified by NIM by using a aperture area of 48.815 mm^2 (Table S2, Figure S7b, and Figure S8).

External quantum efficiency (EQE) measurements were conducted to confirm the J_{SC} of the OSCs. As shown in Figure 3b, the PBDB-T-SF:IT-4F-based device has a broader photon response range than PBDB-T:ITIC-based device (Figure S5b), and a maximum value of 83% was recorded at 570 nm. The integrated current density was 19.81 mA/cm^2 for the PBDB-T-SF:IT-4F-based device, which agrees well with the J−V measurements. The PBDB-T-SF:IT-4F blend film shows higher μ_h and μ_e than that of PBDB-T:ITIC film (Table S1). The exciton dissociation probabilities (P_{diss}) (Figure S9) were calculated to be 93% and 90% for the PBDB-T-SF:IT-4F- and PBDB-T:ITIC-based devices, respectively, indicating that the exciton dissociation and charge collection processes are quite efficient in the OSC devices, especially in PBDB-T-SF:IT-4F-based device.[37]

Then, OSCs were fabricated with different active layer thicknesses from 100−300 nm to investigate the impact of the thickness on the photovoltaic properties of the device (Figure 3c). An increase in the active layer thicknesses does not have a great influence on the V_{OC} of the device, whereas the J_{SC} increases and the FF decreases, resulting in a nearly 10% drop in efficiency when the layer thickness is 200 nm. Notably, PCEs of over 12% can be obtained at the thickness range of 100−200 nm, which is very important for the large-scale fabrication of OSCs via roll-to-roll technology. We then tested the long-term storage stability of the OSCs in an N_2-filled glovebox. As shown in Figure 3d, after over 1700 h of storage, the PBDB-T-SF:IT-4F-based device can still achieve a PCE of 11.99%. The air stabilities of ITIC- and IT-4F-based device without encapsulation have been measured (Figure S10), and the PCE of ITIC- and IT-4F-based devices are 10.22% and 8.16% after 194 h in air condition, while the PCE of PBDB-T-SF:PC71BM-based device decrease from 8.89% to 7.00%. Furthermore, we also tested the optimal device under various light intensity conditions (Figure S11). The OSCs can deliver PCEs of over 12% under different light intensities from 10 to 100 mW/cm^2, with a maximum value of 13.37% obtained at 70 mW/cm^2.

We investigated the surface and bulk morphologies of the blend films by atomic force microscopy (AFM) and transmission electron microscopy (TEM). As shown in Figure 4a,

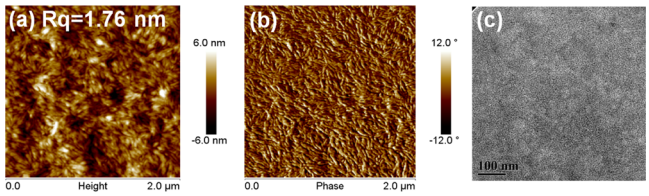

Figure 4. Morphology images of the blend films: AFM (a) height and (b) phase images of PBDB-T-SF:IT-4F and (c) TEM image of the PBDB-T-SF:IT-4F blend film.

the PBDB-T-SF:IT-4F blend film shows a smooth and uniform surface with a root-mean-square surface roughness (R_q) of 1.76 nm. Nanoscale phase separation with appropriate domain sizes was observed in the phase pattern (Figure 4b) and TEM image (Figure 4c) of the blend film, which ensures efficient charge transport in the OSC device. The PBDB-T-SF:IT-4F blend morphology properties are very similar to that of PBDB-T:ITIC blend film (Figure S12).

In conclusion, we applied the synergistic molecular optimization of a donor and acceptor for photovoltaic application in this work. A new polymer donor PBDB-T-SF and small molecule acceptor IT-4F were successfully designed and synthesized via fluorination. The newly designed active materials show down-shifted molecular energy levels relative to their nonfluorinated counterparts. Because of the broad optical absorption range and enhanced absorption coefficient of the active layer, the corresponding OSC device shows an obvious improvement in the J_{SC}. The best device fabricated from PBDB-T-SF:IT-4F yields a remarkable PCE of 13%. Furthermore, the OSC device shows good tolerance toward the active layer thickness and good stability with respect to the efficiency. Our study demonstrates that rational molecular optimization is of great importance to improve the efficiency of OSC, and the OSC commercialization is very promising in the near future.

■ ASSOCIATED CONTENT

Supporting Information

The Supporting Information is available free of charge on the ACS Publications website at DOI: 10.1021/jacs.7b02677.

DOI: 10.1021/jacs.7b02677
J. Am. Chem. Soc. 2017, 139, 7148−7151

Synthesis and characterization of PBDB-T-SF and IT-4F, and device fabrication and measurement (PDF)

AUTHOR INFORMATION

Corresponding Authors

*hjhzlz@iccas.ac.cn
*yaohf@iccas.ac.cn

ORCID

Sunsun Li: 0000-0003-3581-8358
Huifeng Yao: 0000-0003-2814-4850
Jianhui Hou: 0000-0002-2105-6922

Notes

The authors declare no competing financial interest.

ACKNOWLEDGMENTS

The authors acknowledge the financial support from NSFC (91333204, 21325419, 51673201), the Chinese Academy of Sciences (XDB12030200, KJZD-EW-J01), the National Basic Research Program 973 (2014CB643501), and the CAS-Croucher Funding Scheme for Joint Laboratories (CAS14601).

REFERENCES

(1) Dou, L. T.; Liu, Y. S.; Hong, Z. R.; Li, G.; Yang, Y. *Chem. Rev.* **2015**, *115*, 12633.
(2) Li, Y. F. *Acc. Chem. Res.* **2012**, *45*, 723.
(3) Zhang, K.; Hu, Z.; Sun, C.; Wu, Z.; Huang, F.; Cao, Y. *Chem. Mater.* **2017**, *29*, 141.
(4) Nielsen, C. B.; Holliday, S.; Chen, H.-Y.; Cryer, S. J.; McCulloch, I. *Acc. Chem. Res.* **2015**, *48*, 2803.
(5) Thompson, B. C.; Frechet, J. M. J. *Angew. Chem., Int. Ed.* **2008**, *47*, 58.
(6) Guo, X. G.; Zhou, N. J.; Lou, S. J.; Smith, J.; Tice, D. B.; Hennek, J. W.; Ortiz, R. P.; Navarrete, J. T. L.; Li, S. Y.; Strzalka, J.; Chen, L. X.; Chang, R. P. H.; Facchetti, A.; Marks, T. J. *Nat. Photonics* **2013**, *7*, 825.
(7) He, Y. J.; Chen, H. Y.; Hou, J. H.; Li, Y. F. *J. Am. Chem. Soc.* **2010**, *132*, 1377.
(8) Zhang, G.; Zhang, K.; Yin, Q.; Jiang, X.-F.; Wang, Z.; Xin, J.; Ma, W.; Yan, H.; Huang, F.; Cao, Y. *J. Am. Chem. Soc.* **2017**, *139*, 2387.
(9) Li, M.; Gao, K.; Wan, X.; Zhang, Q.; Kan, B.; Xia, R.; Liu, F.; Yang, X.; Feng, H.; Ni, W.; Wang, Y.; Peng, J.; Zhang, H.; Liang, Z.; Yip, H.-L.; Peng, X.; Cao, Y.; Chen, Y. *Nat. Photonics* **2016**, *11*, 85.
(10) Zhao, J.; Li, Y.; Yang, G.; Jiang, K.; Lin, H.; Ade, H.; Ma, W.; Yan, H. *Nat. Energy* **2016**, *1*, 15027.
(11) Deng, D.; Zhang, Y. J.; Zhang, J. Q.; Wang, Z. Y.; Zhu, L. Y.; Fang, J.; Xia, B. Z.; Wang, Z.; Lu, K.; Ma, W.; Wei, Z. X. *Nat. Commun.* **2016**, *7*, 13740.
(12) Koster, L. J. A.; Mihailetchi, V. D.; Blom, P. W. M. *Appl. Phys. Lett.* **2006**, *88*, 093511.
(13) Li, S.; Ye, L.; Zhao, W.; Zhang, S.; Mukherjee, S.; Ade, H.; Hou, J. *Adv. Mater.* **2016**, *28*, 9423.
(14) Holliday, S.; Ashraf, R. S.; Wadsworth, A.; Baran, D.; Yousaf, S. A.; Nielsen, C. B.; Tan, C. H.; Dimitrov, S. D.; Shang, Z. R.; Gasparini, N.; Alamoudi, M.; Laquai, F.; Brabec, C. J.; Salleo, A.; Durrant, J. R.; McCulloch, I. *Nat. Commun.* **2016**, *7*, 11585.
(15) Baran, D.; Ashraf, R. S.; Hanifi, D. A.; Abdelsamie, M.; Gasparini, N.; Rohr, J. A.; Holliday, S.; Wadsworth, A.; Lockett, S.; Neophytou, M.; Emmott, C. J. M.; Nelson, J.; Brabec, C. J.; Amassian, A.; Salleo, A.; Kirchartz, T.; Durrant, J. R.; McCulloch, I. *Nat. Mater.* **2016**, *16*, 363.
(16) Li, S.; Ye, L.; Zhao, W.; Zhang, S.; Ade, H.; Hou, J. *Adv. Energy Mater.* **2017**, 1700183.
(17) Bin, H.; Gao, L.; Zhang, Z.-G.; Yang, Y.; Zhang, Y.; Zhang, C.; Chen, S.; Xue, L.; Yang, C.; Xiao, M.; Li, Y. *Nat. Commun.* **2016**, *7*, 13651.
(18) Meng, D.; Sun, D.; Zhong, C.; Liu, T.; Fan, B.; Huo, L.; Li, Y.; Jiang, W.; Choi, H.; Kim, T.; Kim, J. Y.; Sun, Y.; Wang, Z.; Heeger, A. J. *J. Am. Chem. Soc.* **2016**, *138*, 375.
(19) Dai, S.; Zhao, F.; Zhang, Q.; Lau, T.-K.; Li, T.; Liu, K.; Ling, Q.; Wang, C.; Lu, X.; You, W.; Zhan, X. *J. Am. Chem. Soc.* **2017**, *139*, 1336.
(20) Liu, Y.; Zhang, Z.; Feng, S.; Li, M.; Wu, L.; Hou, R.; Xu, X.; Chen, X.; Bo, Z. *J. Am. Chem. Soc.* **2017**, *139*, 3356.
(21) Lin, Y. Z.; He, Q.; Zhao, F. W.; Huo, L. J.; Mai, J. Q.; Lu, X. H.; Su, C. J.; Li, T. F.; Wang, J. Y.; Zhu, J. S.; Sun, Y. M.; Wang, C. R.; Zhan, X. W. *J. Am. Chem. Soc.* **2016**, *138*, 2973.
(22) Liu, J.; Chen, S.; Qian, D.; Gautam, B.; Yang, G.; Zhao, J.; Bergqvist, J.; Zhang, F.; Ma, W.; Ade, H.; Inganäs, O.; Gundogdu, K.; Gao, F.; Yan, H. *Nat. Energy* **2016**, *1*, 16089.
(23) Lee, C.; Kang, H.; Lee, W.; Kim, T.; Kim, K. H.; Woo, H. Y.; Wang, C.; Kim, B. J. *Adv. Mater.* **2015**, *27*, 2466.
(24) Duan, C.; Zango, G.; García Iglesias, M.; Colberts, F. J. M.; Wienk, M. M.; Martínez-Díaz, M. V.; Janssen, R. A. J.; Torres, T. *Angew. Chem., Int. Ed.* **2017**, *56*, 148.
(25) Xiao, S.; Zhang, Q.; You, W. *Adv. Mater.* **2016**, 1601391.
(26) Zhang, Z.; Li, Y. *Sci. China: Chem.* **2015**, *58*, 192.
(27) Chen, H.; Hou, J.; Zhang, S.; Liang, Y.; Yang, G. W.; Yang, Y.; Yu, L.; Wu, Y.; Li, G. *Nat. Photonics* **2009**, *3*, 649.
(28) (a) Tang, M. L.; Bao, Z. A. *Chem. Mater.* **2011**, *23*, 446. (b) Oh, J.; Kranthiraja, K.; Lee, C.; Gunasekar, K.; Kim, S.; Ma, B.; Kim, B. J.; Jin, S.-H. *Adv. Mater.* **2016**, *28*, 10016.
(29) Zhang, M.; Guo, X.; Zhang, S.; Hou, J. *Adv. Mater.* **2014**, *26*, 1118.
(30) Kawashima, K.; Fukuhara, T.; Suda, Y.; Suzuki, Y.; Koganezawa, T.; Yoshida, H.; Ohkita, H.; Osaka, I.; Takimiya, K. *J. Am. Chem. Soc.* **2016**, *138*, 10265.
(31) Reichenbacher, K.; Suss, H. I.; Hulliger, J. *Chem. Soc. Rev.* **2005**, *34*, 22.
(32) Lu, L.; Yu, L. *Adv. Mater.* **2014**, *26*, 4413.
(33) Stuart, A. C.; Tumbleston, J. R.; Zhou, H.; Li, W.; Liu, S.; Ade, H.; You, W. *J. Am. Chem. Soc.* **2013**, *135*, 1806.
(34) Zhao, W.; Qian, D.; Zhang, S.; Li, S.; Inganas, O.; Gao, F.; Hou, J. *Adv. Mater.* **2016**, *28*, 4734.
(35) Lin, Y.; Wang, J.; Zhang, Z.; Bai, H.; Li, Y.; Zhu, D.; Zhan, X. *Adv. Mater.* **2015**, *27*, 1170.
(36) Yao, H.; Cui, Y.; Yu, R.; Gao, B.; Zhang, H.; Hou, J. *Angew. Chem., Int. Ed.* **2017**, *56*, 3045.
(37) Wu, J. L.; Chen, F. C.; Hsiao, Y. S.; Chien, F. C.; Chen, P. L.; Kuo, C. H.; Huang, M. H.; Hsu, C. S. *ACS Nano* **2011**, *5*, 959.

DOI: 10.1021/jacs.7b02677
J. Am. Chem. Soc. 2017, 139, 7148−7151